RNA-binding protein quaking 5 inhibits the progression of non-small cell lung cancer by upregulating netrin-4 expression

ZHUO WU[1], SHIJUN LIU[1], GESHUO PANG[1] and HONGFANG JIANG[2]

[1]Department of Thoracic Surgery, Fourth Affiliated Hospital of China Medical University, Shenyang, Liaoning 110032; [2]Department of Geriatrics, Shengjing Hospital of China Medical University, Shenyang, Liaoning 110001, P.R. China

Received June 2, 2023; Accepted September 5, 2023

DOI: 10.3892/or.2023.8641

Abstract. It was recently reported that netrin-4 (Ntn-4), a component of the extracellular matrix, when downregulated, is involved in the progression of several types of cancer, including breast cancer, colorectal tumours, neuroblastoma and gastric cancer. In the present study, the level of Ntn-4 was examined in a public non-small cell lung cancer (NSCLC) dataset from the Netherlands Cancer Institute. This analysis revealed that the mRNA expression level of Ntn-4 was lower in the samples of patients with NSCLC compared with that in the control samples. Consistent with the mRNA level, the protein level of Ntn-4 was also found to be decreased in NSCLC cells. However, both the function of Ntn-4 and the underlying mechanisms of Ntn-4 downregulation in NSCLC have yet to be fully elucidated. As was anticipated, the overexpression of Ntn-4 led to a marked decrease in the proliferation, migration and invasion of NSCLC cells. Notably, RNA-binding protein quaking 5 (Qki-5) was found to exhibit antitumor activity in lung cancer, not only by enhancing the level of Ntn-4 by binding to Ntn-4 mRNA, but also by suppressing the proliferation, invasion and migration of NSCLC cells. However, Qki-5 is known to be frequently downregulated in NSCLC. Moreover, the knockdown of Ntn-4 was found to reverse the suppressive effects of Qki-5 on NSCLC progression both *in vitro* and *in vivo*. Taken together, the findings of the present study demonstrate that Ntn-4 is able to suppress the progression of NSCLC, and that the level of Ntn-4 can be regulated by Qki-5. Therefore, Ntn-4 may be a novel diagnostic and therapeutic target for the treatment of NSCLC.

Correspondence to: Professor Hongfang Jiang, Department of Geriatrics, Shengjing Hospital of China Medical University, 36 Sanhao Street, Heping, Shenyang, Liaoning 110001, P.R. China
E-mail: jianghf@sj-hospital.org

Key words: non-small cell lung cancer, netrin-4, RNA-binding protein quaking, migration, invasion

Introduction

Non-small cell lung cancer (NSCLC) accounts for ~85% of all cases of lung cancer, and can be further classified as lung adenocarcinoma (LUAD), lung squamous cell carcinoma (LUSC) and large cell carcinoma (1). However, the majority of lung cancer cases are diagnosed at a late stage after tumour cell metastasis has usually occurred, which leads to a poor prognosis and high mortality rates worldwide (2). Therefore, identifying biomarkers for the early diagnosis of lung cancer and therapeutic targets are essential in order to enhance clinical outcomes.

The netrin (Ntn) family consists of Ntn-1, -2, -3, -4, -G1 and G2, which all belong to the superfamily of laminins. These proteins were initially described as chemoattractive or chemorepulsive cues to guide axonal migration and neuronal growth in the developing central nervous system (3,4). Over the course of the past few decades, Ntns have been shown to be involved in diverse biological processes other than neuronal development, including processes such as organogenesis, angiogenesis, tumorigenesis and inflammation (5,6). Ntn-4 was cloned in 2000 and has been found to be involved in several different types of cancer. Ntn-4 was shown to inhibit angiogenesis and the progression of colorectal cancer by binding to the cell-surface receptor, neogenin, or uncoordinated receptor 5 (Unc5) (7-10); by contrast, other studies have reported that Ntn-4 promotes the proliferation and invasion of gastric cancer cells (11), and it has also been shown to increase the survival and migration rates of neuroblastoma cells (12), suggesting that the role of Ntn-4 in tumour progression remains controversial. Previously, Reuten *et al* (13) demonstrated that Ntn-4 plays a key role in regulating basement membrane (BM) composition and stiffness by interacting with the γ1 chain of laminin, rather than binding to any of the Ntn receptors. It has also been demonstrated that the presence of Ntn-4 maintains a softer BM, and a decrease in the level of Ntn-4 leads to an increase in BM stiffness and the alteration of the tumour microenvironment, which consequently promotes the migration and metastasis of breast cancer cells (14,15). The level of Ntn-4 in breast cancer tumours has been found to be associated with a longer disease-free survival and overall survival rates, and it has been shown to be an independent prognostic factor in patients with early-stage breast cancer (16,17). Data from a public NSCLC dataset from the Netherlands Cancer Institute (NKI) revealed

that there was a 1.5-fold decrease in the expression level of Ntn-4 in patients with NSCLC; however, the biological effects of Ntn-4 on NSCLC have yet to be fully elucidated. Moreover, the precise reason why Ntn-4 is downregulated in NSCLC needs to be further investigated.

Owing to alternative splicing, the RNA-binding protein quaking (Qki) gene is translated into three main protein isoforms, namely Qki-5, Qki-6 and Qki-7, which differ in terms of their C-terminal amino acid sequences (18). Qki regulates the post-transcriptional level of target genes through selectively interacting with the Qki response element (19). Increasing evidence has revealed that Qki fulfils an important role in lung cancer as a tumour suppressor by alternatively splicing cancer-associated genes. Notably, a low expression level of Qki in NSCLC is an independent prognostic factor for disease-free survival (20). It has also been reported that a low expression level of Qki-6 is positively associated with poor overall survival rates in patients with NSCLC. The upregulation of Qki-6 expression has been found to inhibit NSCLC cell□proliferation, migration and epithelial-mesenchymal transition (EMT) (21). The overexpression of Qki-5 has also been shown to suppress the progression and EMT of NSCLC cells by inhibiting the level of β-catenin (22), the inhibition of Notch signalling (23) and TGF-β/Smad signalling (24), or by alternatively repressing the splicing of the cytoskeletal gene adducin3 in lung cancer cells (25).

Since low levels of Qki-5 and Ntn-4 have been shown to contribute to the development and progression of NSCLC, the present study aimed to investigate whether Qki-5 can affect NSCLC progression by regulating the expression of Ntn-4. To address this question, the correlation between Qki-5 and Ntn-4 was first analysed according to the NKI data. As was anticipated, Qki-5 and Ntn-4 were found to be strongly correlated in NSCLC. Subsequently, as detailed in the Materials and methods section, a series of experiments were performed which confirmed that a decrease in the level of Qki-5 promoted the proliferation, migration, invasion and EMT of NSCLC by downregulating Ntn-4. Taken together, the findings of the present study shed light onto the biological role of Ntn-4 in NSCLC progression, also helping to elucidate one of the underlying mechanisms responsible for the downregulation of Ntn-4 in lung cancer.

Materials and methods

The Cancer Genome Atlas (TCGA) data analysis. TCGA data analysis was performed using the publicly accessible TCGA database (https://tcga-data.nci.nih.gov/tcga/). The mRNA values of Ntn-4 and Qki were collected from the samples of 483 patients with LUAD and 59 control samples, and from the samples of 486 patients with LUSC and 50 control samples, which were subsequently quantified according to TCGA normalization protocol. The mRNA levels of Qki and Ntn-4 that were associated with the survival data for the patients with LUAD and LUSC were also analysed according to TCGA datasets.

Clinical sample collection. For the Ntn-4 and Qki-5 mRNA expression level analysis, a total of 30 patients diagnosed with LUAD, and 30 patients diagnosed with LUSC, at the Fourth Affiliated Hospital of China Medical University were enrolled in the present study. The Ethics Committee of the Fourth Hospital of China Medical University approved the present study (approval no. EC-2018-HX-013), and all the patients involved in this research signed informed consent forms. Tumour tissues, and the corresponding adjacent normal tissues were dissected and stored in liquid nitrogen for periods up to 90 days prior to performing the reverse transcription-quantitative PCR (RT-qPCR) experiments.

Immunohistochemistry (IHC). The tumour samples from patients with LUAD or LUSC were collected between July, 2018 and August, 2019. For the Ntn-4 and Qki-5 IHC staining of the human LUAD and LUSC tissues, slides were prepared using an ultrathin semiautomatic microtome, deparaffinized in 100% xylene and rehydrated in a graded ethanol series (70, 80, 90, 95 and 100%, Beijing InnoChem Science & Technology Co.,Ltd.). For antigen retrieval, the slides were treated with sodium citrate solution (pH 6.0) (Beijing Solarbio Science & Technology Co., Ltd.) for 6 min at 100˚C. After incubating the slides in 1% bovine serum albumin in phosphate-buffered saline (PBS) for 30 min at room temperature, the slides were incubated with anti-Ntn-4 (rabbit, 1:1,000, cat. no. NBP191343, Novus Biologicals, LLC) and anti-Qki-5 (rabbit, 1:1,000, cat. no. AB9904, MilliporeSigma) antibodies overnight at 4˚C. After washing the slides several times with PBS, they were incubated with a goat anti-rabbit IgG secondary antibody conjugated to horseradish peroxidase (HRP; 1:300, cat. no. BF03008, Biodragon Immunotech) for 30 min at room temperature. Staining was visualized using a DAB Horseradish Peroxidase Color Development kit (p0203, Beyotime Institute of Biotechnology). An appropriate amount of DAB dyeing solution was then added, and the tissues were fully covered and incubated at room temperature for 30 min away from light. The nuclei were counterstained for 30 sec with haematoxylin at room temperature. (C0107, Beyotime Institute of Biotechnology) For the negative control experiments, sections were incubated with PBS instead of the primary antibodies. Positive staining controls were performed using para-carcinoma tissues of breast cancer and renal cancer. The slides were finally covered with neutral balata and cover glass slips. The qualitative scoring system used for evaluation of the intensity of staining was as follows: Negative (no staining, 0); weakly positive (+); moderately positive (++); and strongly positive (+++). Images of the stained tissues were obtained using a positive fluorescence microscope (BX53/DP73, Olympus Corporation).

Cells, cell culture and treatment. The human LUAD cell lines, A549 (cat. no. TCHu150) and H23 (cat. no. SCSP-5002) were purchased from The Cell Bank of Type Culture Collection of the Chinese Academy of Sciences (Shanghai, China). The LUSC cell line, NCI-H2107 (cat. no. CRL-5983_FL), and the human bronchial epithelial cell line, 16HBE (cat. no. PCS-300-010) were purchased from Jennino Biological Technology (Guangzhou, China). The cells were cultured in Gibco® Roswell Park Memorial Institute (RPMI)-1640 medium (Thermo Fisher Scientific, Inc.) supplemented with 10% (v/v) Gibco® foetal bovine serum (FBS; Thermo Fisher

Scientific, Inc.) and maintained in a humidified atmosphere with 5% CO_2 at 37˚C.

Lentiviral production and transfection. To generate the Ntn-4- and Qki-5-overexpressing cell lines (oe-Ntn-4 and oe-Qki-5), the Ntn-4 or Qki-5 coding sequence, respectively, was cloned into the GV492 (11.9 kb) lentiviral vector (Shanghai Genechem Co., Ltd.) to form recombinant plasmids. Subsequently, the recombinant GV492, Helper 1.0 (12.0 kb) and Helper 2.0 (5.8 kb) plasmids were co-transfected into 293T cells (Wuhan Procell Life Technology Co., Ltd.). After 48 or 72 h, the culture supernatant was harvested, concentrated and purified (82,700 g for 2 h at 4˚C). The concentrations of lentivirus were measured using Immunostaining Plaque Assay (26), and the data obtained revealed that the titres of LV-Ntn-4 and LV-Qki-5 were $1.5E^{+09}$ and $1.2E^{+09}$ (TU/ml), respectively.

To produce the short hairpin RNAs (shRNAs) of human Ntn-4 and Qki-5, the target genes for Ntn-4 (sh-Ntn-4) (sequence, 5'-CCGGGCGCTATTTGTACTTCTAAAT-3'), Qki-5 (sh-Qki-5) (sequence, 5'-CCGGCTATTAACCCACAG CATTTT-3') and the negative control (NC) scramble (sh-NC, the scramble sequences of shNtn-4 and shQki-5 are TTC TCCGAACGTGTCACGT and TATTAACCACAATGCGCT TTGCCC, respectively) were inserted into the GV118 vector (7.4 kb) (Shanghai Genechem Co., Ltd.). The recombinant plasmids Helper 1.0 (12.0 kb) and Helper 2.0 (5.8 kb) were again co-transfected into 293T cells. The production and quantification of LV-Ntn-4-RNAi were performed following the protocol described above (26). The titre of LV-Ntn-4-RNAi was determined to be $2.00E^{+08}$ TU/ml. Lentiviral production was performed by Shanghai Genechem Co., Ltd. Finally, the cells (~$1x10^5$ cells/ml) were seeded in cell culture dishes and subsequently transfected with the lentivirus, following the manufacturer's instructions.

Cell viability analysis. The transfected A549 and H2107 cells were seeded into 96-well plates at a density of $4x10^3$ cells/well, and allowed to grow for 2 days. Cell proliferation was determined using a Cell Counting Kit-8 (CCK-8) (Beyotime Institute of Biotechnology) assay. The absorbance at 450 nm was read using a microplate reader (BioTek Instruments, Inc.).

RT-qPCR analysis. Total RNA was extracted using Invitrogen® TRIzol™ reagent (Thermo Fisher Scientific, Inc.), and first-strand cDNA was generated using an RT system in a 20 μl reaction mixture [SYBR-Green Master Mix (2X) (No ROX) 10 μl, PCR forward primer (10 μM) 0.4 μl, PCR reverse primer (10 μM) 0.4 μl, DNA 2 μl and ddH_2O 7.2 μl] containing 1 μg total RNA. Aliquots (0.5 μl) of cDNA were amplified using Fast SYBR-Green PCR Master Mix (Vazyme Biotech Co., Ltd.) in each 20 μl reaction. PCRs were run on a Roche Light Cycler 480 II with the following primers: Qki-5 forward, 5'-TCCGAGGCAAAGGCTCAATGAG-3' and reverse, 5'-GCTCTGTTCTGAGCATCTTCCAC-3'; Ntn-4 forward, 5'-GTACTTTGCGACTAACTGCTCC-3' and reverse, 5'-TCC AGTGCATGGAAAAGGACT-3'; and GAPDH forward, 5'-GAAGGTGAAGGTCGGAGT-3' and reverse, 5'-GAAGAT GGTGATGGGATTTC-3'. The PCR thermocycling conditions were pre-denaturation for 30 sec at 95˚C, denaturation for 20 sec at 95˚C, annealing for 15 sec at 58˚C, and extension for 15 sec at 72˚C. The relative expression values of Qki-5 and Ntn-4 were calculated and normalized to those of GAPDH in each sample using the $2^{-\Delta\Delta Cq}$ method (27).

Western blot analysis. Following transfection of the cells for 48 h, the cells were collected, washed and lysed with cell lysis buffer (P0013B, Beyotime Institute of Biotechnology) containing protease inhibitors phenylmethylsulfonyl fluoride (PMSF; ST506-2, Beyotime Institute of Biotechnology), and the protein concentrations were quantified using an enhanced BCA protein assay kit (Biosharp Life Sciences). Protein electrophoresis was performed using 10% sodium dodecyl sulphate-polyacrylamide gel electrophoresis (SDS-PAGE; kgb113k, Nanjing KeyGen Biotech Co., Ltd.), and western blotting was performed on a nitrocellulose transfer membrane. After using 5% skimmed milk powder closed 2 h at room temperature, the nitrocellulose filter membranes (66485, Pall Life Sciences) were incubated at 4˚C overnight with the following primary antibodies: Anti-β-actin (mouse, 1:5,000; cat. no. 66009-1-Ig, Proteintech Group, Inc.), anti-Ntn-4 (rabbit, 1:1,000; cat. no. NBP191343, Novus Biologicals, LLC), anti-Qki-5 (rabbit, 1:1,000; cat. no. AB9904, MilliporeSigma), anti-E-cadherin (rabbit, 1:5,000; cat. no. 20874-1-AP), anti-N-cadherin (rabbit, 1:5,000; cat. no. 22018-1-AP), anti-vimentin (rabbit, 1:5,000; cat. no. 13066-1-AP) and anti-Snail (rabbit, 1:500; 13099-1-AP) (all from Proteintech Group, Inc.). After washing three times with Tris-buffered saline containing Tween (TBST; cat. no. t917680; Beijing Innochem Technology Co., Ltd), the membranes were incubated with HRP-conjugated secondary antibody (Goat anti-Rabbit, 1:5000; cat. no. A21020; Abbkine Scientific Co., Ltd.) at room temperature for 2 h. The protein bands were scanned using an Odyssey infrared imager (LI-COR Biosciences). The relative grey values of the proteins of interest were analysed using ImageJ software (Version 1.51j8, National Institutes of Health) and normalized against those of β-actin.

Wound healing assay. The transfected A549 and H2107 cells were grown until they had reached ~90% confluency in a 12-well plate, and a cell wound was created by scratching the cells with a sterile 200-μl pipette tip. After washing the cells with PBS twice, they were cultured in RPMI-1640 medium supplemented with 0.5% FBS for 48 h. Cell images were captured under a microscope (IX73, Olympus Corporation). The gap sizes were measured using ImageJ software (version 1.51J8) and calculated as the percentages after 48 h relative to the gap sizes at 0 h.

Cell migration assay. The cells were collected and resuspended in RPMI-1640 medium (Thermo Fisher Scientific, Inc.). Aliquots (200 μl) of cell suspension were placed in the upper chamber of a Transwell insert (Corning, Inc.). Subsequently, the Transwell chamber was inserted into a 24-well plate. Following incubation of the cells in RPMI-1640 medium containing 10% (v/v) FBS for 24 h at 37˚C, the cells on the upper membrane of the insert were gently removed using a cotton swab, whereas those cells that had migrated to the bottom surface were fixed with cold methanol (Wuhan Servicebio Co.,Ltd) and stained with crystal violet (Wuhan Servicebio Co., Ltd.) for 30 min at room temperature. Finally,

the cell numbers on the bottom surface were photographed and quantified using an inverted microscope system (Olympus IX73; Olympus Corporation).

RNA immunoprecipitation (RIP) assay. RIP experiments were performed according to the manufacturer's instructions using the BersinBio™ RIP kit (Guangzhou Bersinbio Co., Ltd.). Briefly, the A549 cells were lysed using RIP lysis buffer, and the cell extract was incubated with protein A/G agarose beads (Guangzhou Bersinbio Co., Ltd.) conjugated with either Qki-5 antibody (rabbit, 1:400; cat. no. AB9904, MilliporeSigma) or control IgG (rabbit, 1:4000; cat. no. abs20035, Absin) for 2 h. To purify RNA from the immunoprecipitation, the beads were washed, and the proteins were removed using Proteinase K (0.5 mg/ml). Subsequently, RT-qPCR experiments were performed to analyse the mRNA expression level of Ntn-4.

Xenograft tumour growth. BALB/c (nu/nu) nude female mice (6 weeks old, weighing 20-23 g, n=20 for one trial) were randomly divided into four groups with 5 mice in each group as follows: The oe-NC, oe-Qki-5 + sh-NC, oe-Qki-5 + sh-Ntn-4 and oe-Qki-5 + oe-Ntn-4. The A549 cells ($1x10^7$ cells/ml, 0.2 ml) stably transfected with the vectors overexpression (oe)-Qki-5, oe-Qki-5 and oe-Ntn-4, oe-Qki-5 and sh-Ntn-4, or empty vector were subcutaneously injected into the flanks of mice. During the procedure, the mice were anaesthetised using 4% isoflurane (Shandong Keyuan Pharmaceutical Co.; in oxygen), with the subsequent maintenance of anaesthesia with 2.5% isoflurane. Tumour diameters were measured using callipers, and volumes were calculated based on the formula $V= (a \times b^2)/2$, where a and b represent the longest and the shortest diameter of the tumour, respectively. To minimize animal suffering, the mice were housed under standard conditions and cared for (23˚C; 50% humidity; 12:12 light/dark cycle; food and water were available *ad libitum*) according to institutional guidelines. At the end of the experiment, the animals were euthanized with 5% isoflurane inhalation for 5-10 min; the vital signs were checked to ensure their disappearance, and cervical dislocation was finally performed to avoid the possibility of recovery. Finally, the tumours were isolated, weighed and photographed. The animal experiments were approved by the Animal Research Ethics Committee of the Animal Centre of Shengjing Hospital affiliated with China Medical University (No. KT201945).

Statistical analysis. Statistical analyses were performed using GraphPad Prism version 8.0.0 for Windows by observers blinded to the experimental design. The data are presented as the mean ± standard error of the mean (SEM). The data between two groups were compared using an unpaired ttest, whereas oneway analysis of variance (ANOVA) followed by the post-hoc Tukey's Student Range (HSD) test was adopted for data comparisons among multiple groups. The correlation between the mRNA expression levels of Qki-5 and Ntn-4 was analysed using Pearson's correlation (R^2 correlation). The optical density values and tumour volume at different time points were compared by twofactor ANOVA. A value of $P<0.05$ was considered to indicate a statistically significant difference.

Results

Expression of Ntn-4 is downregulated in NSCLC tissues and cells. The NSCLCassociated expression dataset was retrieved from TCGA database (https://portal.gdc.cancer.gov/). A total of 1,078 samples were obtained, including 483 LUAD samples and 59 control samples, as well as 486 LUSC samples and 50 control samples. The Ntn-4 expression data were subsequently obtained and analysed, and the results confirmed that the mRNA expression level of Ntn-4 was lower in both the LUAD and LUSC samples compared with the control samples (Fig. 1A). No statistically significant differences in the overall survival of the patients with LUSC were observed when comparing between the high and low Ntn-4 mRNA level groups (Fig. 1B); however, the patients with LUAD with a low mRNA expression level of Ntn-4 exhibited poorer overall survival rates compared with the patients with high Ntn-4 mRNA expression levels (Fig. 1C). In addition, the results of RT-qPCR revealed that the expression of Ntn-4 in NSCLC tissues was lower compared with that in the control tissues (Fig. 1D). Moreover, IHC staining analysis also revealed comparatively lower expression levels of Ntn-4 in NSCLC tissues relative to the control tissues (Fig. 1E). With respect to the *in vitro* experiments, the expression level of Ntn-4 was detected in the human NSCLC cell lines, H23, A549 and H2170, and Ntn-4 was found to be expressed at low levels in the human NSCLC cell lines compared with the 16HBE control cell line (Fig. 1F). Moreover, the western blot analysis revealed that, compared with that in the control cells, the Ntn-4 protein expression levels in the NSCLC cells were lower (Fig. 1G).

Ntn-4 inhibits the proliferation, migration and invasion of NSCLC cells. To further examine the effects of Ntn-4 on NSCLC cells, the A549 and H2170 cells were transfected with Ntn-4 shRNA or Ntn-4 overexpression lentivirus. The results from the ensuing RT-qPCR and western blot analysis experiments confirmed that the levels of Ntn-4 were increased in the cells with the lentivirus-mediated overexpression of Ntn-4 compared with the control cells (Fig. 2A and B), whereas the levels were decreased in both the A549 and H2170 cells with Ntn-4 shRNA lentivirus transfection (Fig. 2C and D). The OD values of both A549 (Fig. 2E) and H2170 (Fig. 2F) cells were found to be significantly increased in the sh-Ntn-4 group compared with the sh-NC group, although they were decreased in the cells transfected with the oe-Ntn-4 lentivirus compared with the cells transfected with oe-NC lentivirus, indicating that Ntn-4 may exert its effect through the inhibition of NSCLC cell proliferation. Cell migration and invasion were subsequently assessed using wound healing and Transwell assays. The quantification of the resultant data revealed that the efficiency of scratch wound healing was lower in the cells transfected with oe-Ntn-4 compared with the cells transfected with oe-NC, whereas Ntn-4 silencing led to the opposite findings in terms of the scratch wound healing ability of the cells (Fig. 2G and H). Moreover, the numbers of invading cells were also reduced upon transfection with the oe-Ntn-4 vector compared with sh-NC transfection (Fig. 2I). Collectively, these data suggested that Ntn-4 can reduce the migratory and invasive capabilities of the NSCLC cells.

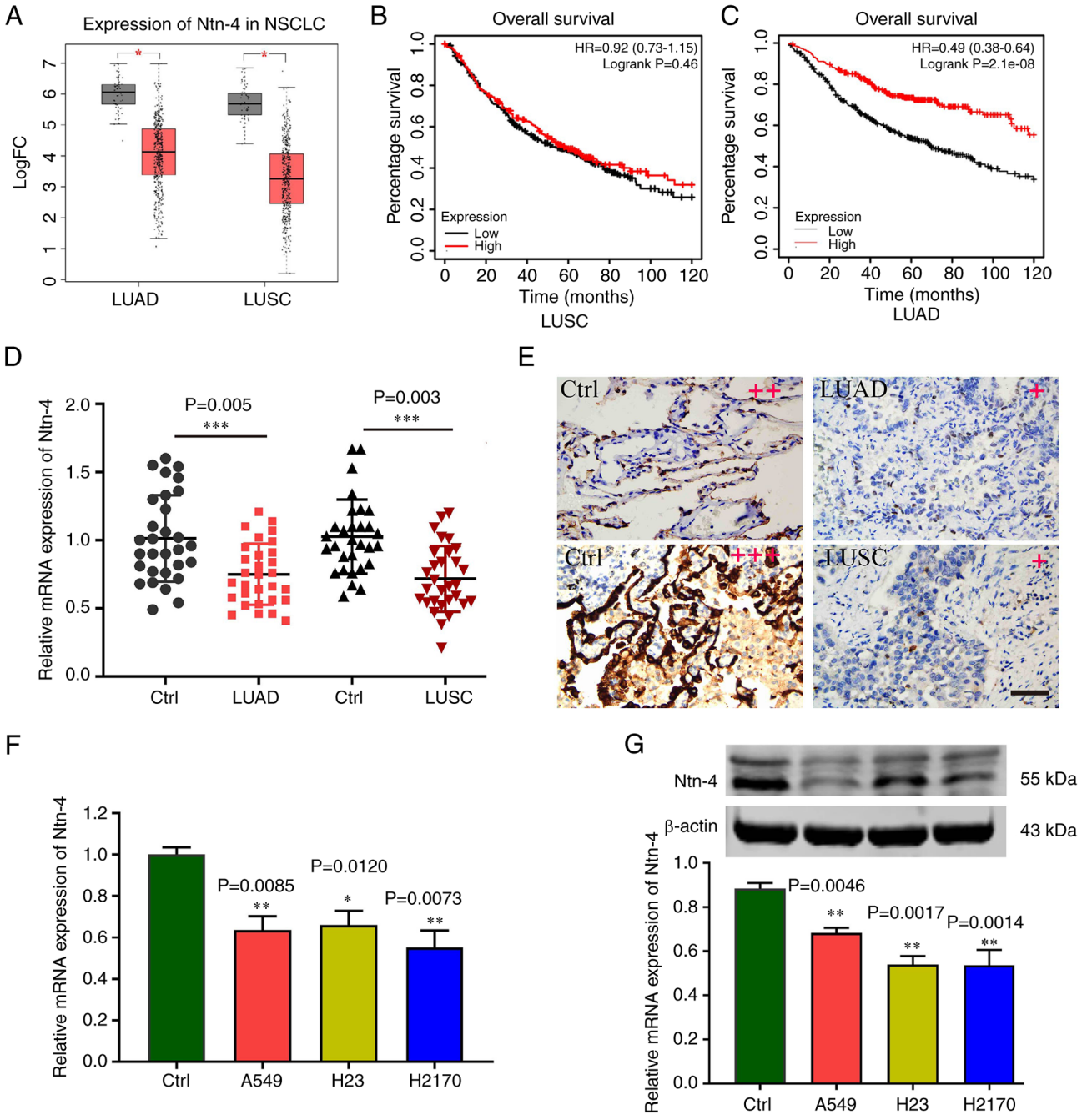

Figure 1. Level of Ntn-4 is decreased in NSCLC tissues and cells. (A) Box-plot of Ntn-4 expression in the LUAD and LUSC datasets; the red boxes portray the cancer groups and the grey boxes represent the control groups. *P<0.05 vs. the control. (B and C) The differences in the overall survival rates between the high and low Ntn-4 mRNA expression level groups in patients with NSCLC are shown. (D) Expression of Ntn-4 mRNA in LUAD and LUSC tissues and adjacent normal tissues (Ctrl) detected using RT-qPCR (n=30). ***P<0.001 vs. Ctrl. (E) Representative images of Ntn-4 immunohistochemical staining in LUAD, LUSC and Ctrl tissues are shown. Scale bar, 100 μm. The qualitative score for staining was as follows: Negative (0: no staining), weakly positive (+), moderate positive (++), and strongly positive (+++). (F) The expression of Ntn-4 mRNA in LUAD cells (NCI-H23 and A549 cell lines), LUSC cells (H2170 cell line) and normal human bronchial epithelial cells (16HBE cell line) was measured using RT-qPCR. Data are presented as the mean ± SEM of three independent experiments (n=3). *P<0.05 and **P<0.01 vs. 16HBE cells (Ctrl). (G) Levels of Ntn-4 protein in LUAD, LUSC and Ctrl cells were detected using western blot analysis, and were quantified using ImageJ software and normalized against β-actin. LUAD, lung adenocarcinoma; LUSC, lung squamous cell carcinoma; NSCLC, non-small cell lung cancer; Ntn, netrin; Ctrl, control; RT-qPCR, reverse transcription-quantitative PCR.

Qki-5 increases the expression of Ntn-4 in NSCLC cells. According to the LUAD and LUSC datasets, the mRNA expression level of Qki was lower in the LUAD and LUSC tissue samples compared with the control samples (Fig. 3A). No statistically significant differences in the overall survival of patients with LUSC were observed comparing between the high and low Qki mRNA level groups; however, patients with LUAD with a low mRNA expression level of Qki exhibited poorer overall survival rates compared with those with high Qki mRNA expression levels (Fig. S1). RT-qPCR experiments were subsequently performed to further confirm that the mRNA expression level of Qki-5 was lower in NSCLC tissues compared with that in the adjacent tissues (Fig. 3B). Furthermore, the IHC staining experiments also revealed a

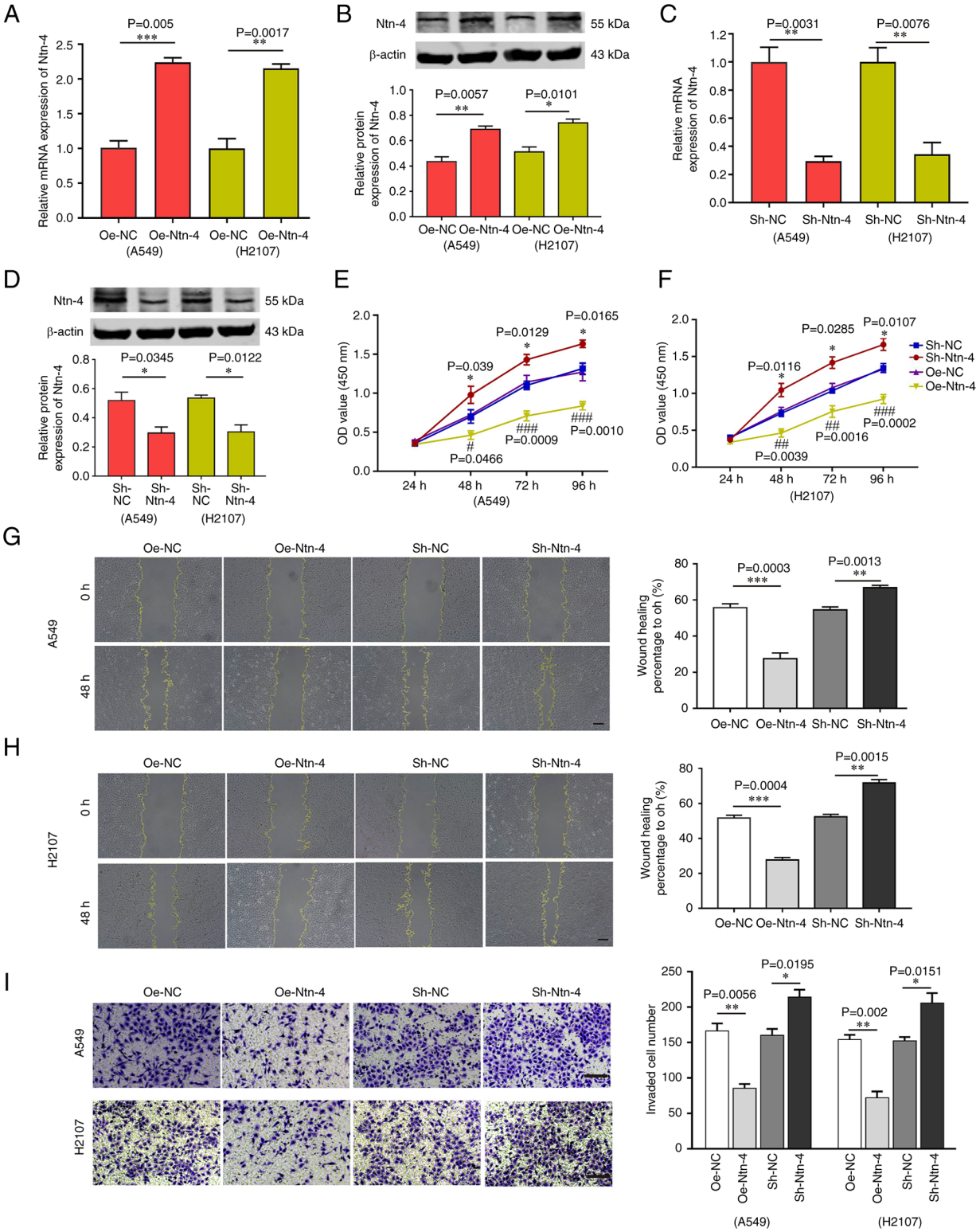

Figure 2. Ntn-4 inhibits the proliferation, migration and invasion of NSCLC cells. (A and B) The mRNA and protein levels of Ntn-4 in NSCLC cells transfected with oe-Ntn-4 lentivirus were detected using RT-qPCR and western blot analysis (n=3). (C and D) The mRNA and protein levels of Ntn-4 in NSCLC cells transfected with Ntn-4 shRNA lentivirus were measured using RT-qPCR and western blot analysis (n=3). (E and F) The proliferation of A549 and H2170 cells was analysed using a CCK-8 assay (n=6). (G and H) A scratch wound assay was used to examine the cell migration capability (n=3). Scale bar, 100 μm. (I) Representative images of Transwell-based cell invasion of NSCLC cells are shown, in addition to the quantification of the number of invaded cells (n=3). Scale bar, 100 μm. Data are presented as the mean ± SEM of three independent experiments. *P<0.05, **P<0.01 and ***P<0.001, vs. shRNA negative control (sh-NC); $^{\#}$P<0.05, $^{\#\#}$P<0.01 and $^{\#\#\#}$P<0.001, vs. overexpression negative control (oe-NC); NSCLC, non-small cell lung cancer; Ntn, netrin; RT-qPCR, reverse transcription-quantitative PCR.

low level of Qki-5 in NSCLC tissues compared with the adjacent normal tissues (Fig. 3C). Relative to the control cells, the mRNA expression level of Qki-5 was also decreased in NSCLC cell lines (Fig. 3D). To clarify the association between Qki-5

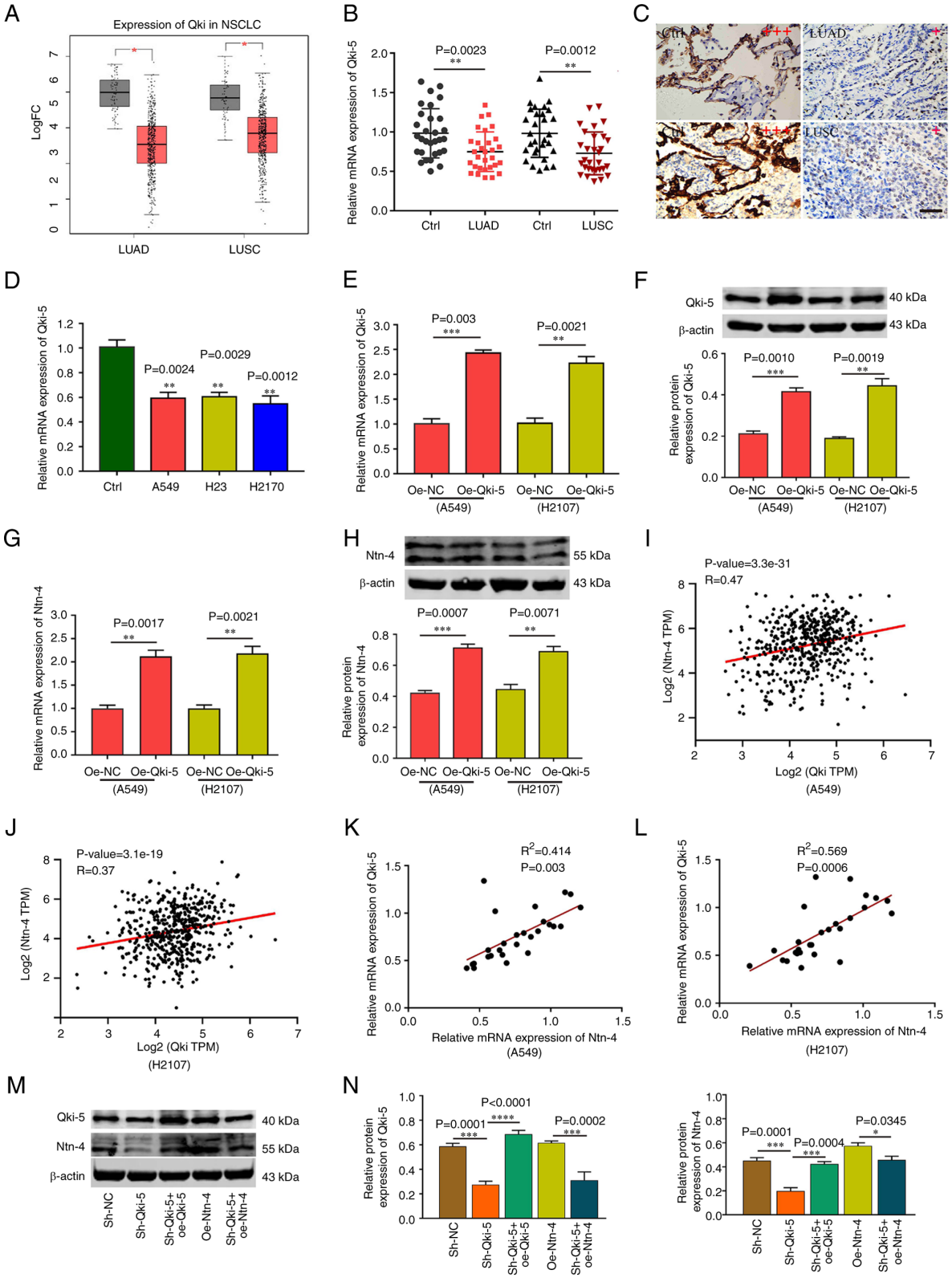

Figure 3. Qki-5 increases the expression of Ntn-4 in NSCLC cells. (A) Box-plot of Qki-5 expression in the LUAD and LUSC datasets; the red boxes represent the cancer groups and the grey boxes represent the control groups. *P<0.05 vs. control (Ctrl). (B) The expression of Qki-5 mRNA in LUAD and LUSC tissues and adjacent normal tissues was measured using RT-qPCR (n=30). **P<0.01 vs. Ctrl. (C) Representative images of immunohistochemical staining for Qki-5 in LUAD and LUSC tissues and adjacent normal tissues are shown. Scale bar, 100 μm. (D) mRNA Expression of Qki-5 in NSCLC cells. Data are presented as the mean ± SEM of three independent experiments (n=3). **P<0.01 vs. Ctrl. (E and F) The mRNA and protein expression levels of Qki-5 were detected using RT-qPCR and western blot analysis, respectively. Data are presented as the mean ± SEM of three independent experiments (n=3). **P<0.01 and ***P <0.001 vs. the oe-NC group. (G and H) The levels of Ntn-4 mRNA and protein were detected using RT-qPCR and western blot analysis. Data are presented as the mean ± SEM of three independent experiments (n=3). **P<0.01 and ***P<0.001 vs. the oe-NC group. (I and J) Expression correlation diagram of Qki-5 and Ntn-4 in the LUAD and LUSC datasets. (K and L) Correlation analysis of Qki-5 and Ntn-4 in the LUAD and LUSC tissues, as determined using Pearson's correlation analysis. (M and N) Protein levels of Qki-5 and Ntn-4 were detected in 16HBE cells using western blot analysis. Data are presented as the mean ± SEM of three independent experiments (n=3). *P<0.05, ***P<0.001 and ****P<0.0001. LUAD, lung adenocarcinoma; LUSC, lung squamous cell carcinoma; NSCLC, non-small cell lung cancer; Ntn, netrin; Qki, quaking; Ctrl, control; RT-qPCR, reverse transcription-quantitative PCR.

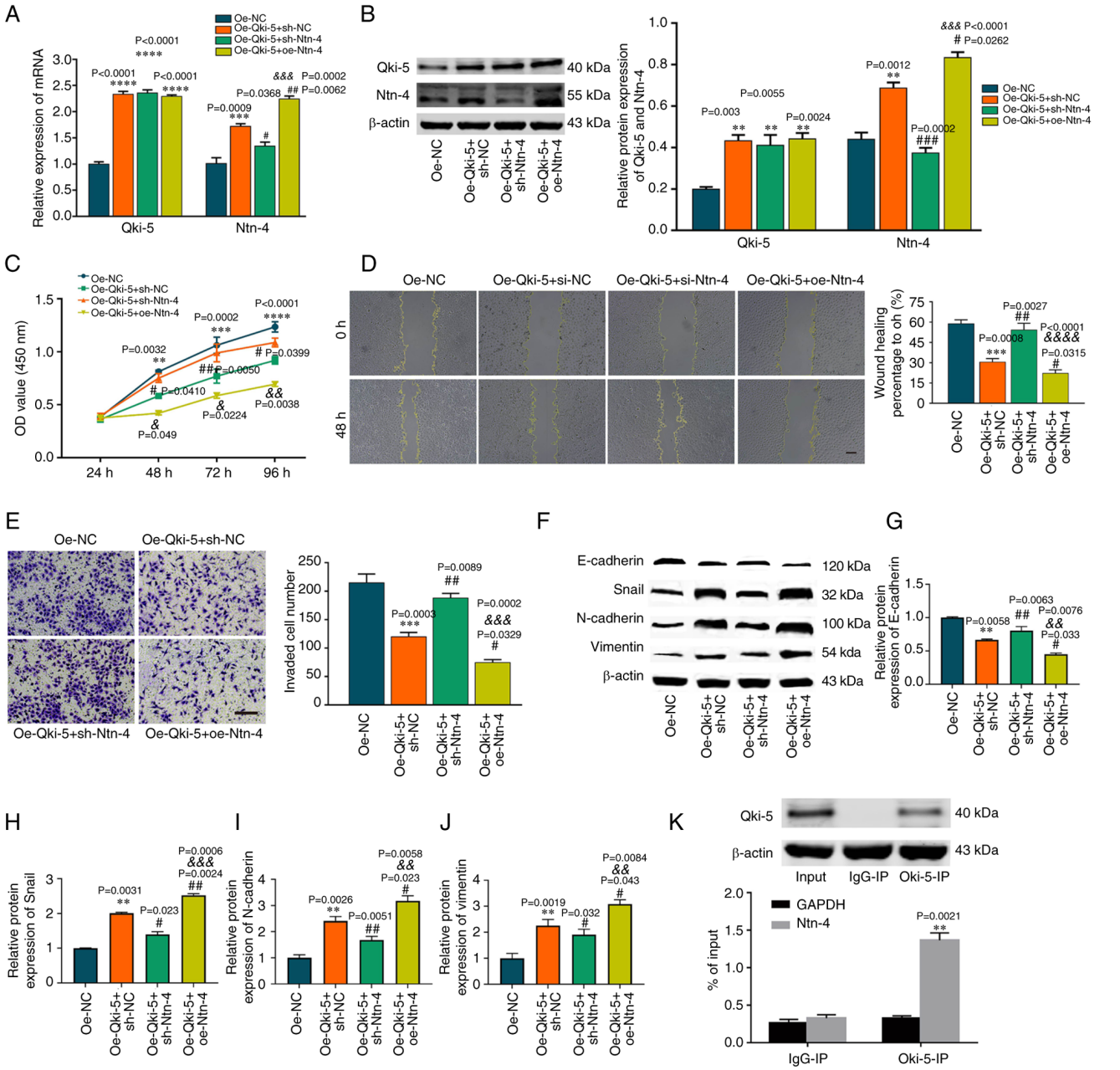

Figure 4. Qki-5 inhibits the progression of NSCLC cells by upregulating Ntn-4. (A) A549 cells were transfected with oe-Qki-5, either alone or combined with oe-Ntn-4 or sh-Ntn-4 lentivirus. mRNA levels of Qki-5 and Ntn-4 were detected using reverse transcription-quantitative PCR (n=3). (B) The protein levels of Qki-5 and Ntn-4 in A549 cells were measured using western blot analysis (n=3). (C) Cell proliferation was detected using a CCK8 assay (n=6). (D) The cell migratory capability of the cells was tested using a scratch wound healing assay (n=3). Scale bar, 100 μm. (E) Transwell assays were used to analyse the cell invasive capability (n=3). Scale bar, 100 μm. (F-J) The EMT marker molecules E-cadherin, N-cadherin, vimentin and Snail were detected by western blotting, and subsequently quantified (n=3). (K) RIP assay was used to confirm the interaction between Qki-5 and Ntn-4. Data are presented as the mean ± SEM of three independent experiments. **P<0.01, ***P<0.001, ****P<0.0001, vs. overexpression negative control (oe-NC); $^{\#}$P<0.05, $^{\#\#}$P<0.01 and $^{\#\#\#}$P<0.001, vs. overexpression Qki-5 and shRNA negative control (oe-Qki-5+sh-NC); $^{\&\&}$P<0.01, $^{\&\&\&}$P<0.001 and $^{\&\&\&\&}$P<0.0001, vs. overexpression Qki-5 and shRNA Ntn-4 (oe-Qki-5+sh-Ntn-4); NSCLC, non-small cell lung cancer; Ntn, netrin; Qki, quaking; EMT, epithelial-mesenchymal transition; RIP, radioimmunoprecipitation.

and Ntn-4, the NSCLC cells were subsequently transfected with oe-Qki-5 lentivirus. The mRNA and protein levels of Qki-5 were found to be markedly upregulated in the A549 and H2170 cells transfected with oe-Qki-5 compared with the cells that were transfected with oe-NC lentivirus (Fig. 3E and F). As was anticipated, the expression of Ntn-4 was upregulated in the oe-Qki-5 cells (Fig. 3G and H). Furthermore, the degree of correlation between Qki-5 and Ntn-4 in the LUAD and LUSC datasets was analysed, and the level of Qki-5 was found to be positively correlated with the level of Ntn-4 (Fig. 3I and J). Pearson's correlation analysis also confirmed that the level of Qki-5 positively correlated with that of Ntn-4 in clinical samples of NSCLC (Fig. 3K and L). To provide further evidence that Qki-5 may be responsible for regulating Ntn-4, Qki-5 was silenced in 16HBE cells, where both Qki-5 and Ntn-4 had been overexpressed. In these experiments, the Ntn-4 protein levels were found to be downregulated in the cells in which Qki-5 was knocked down, even though Qki-5 and Ntn-4 had been

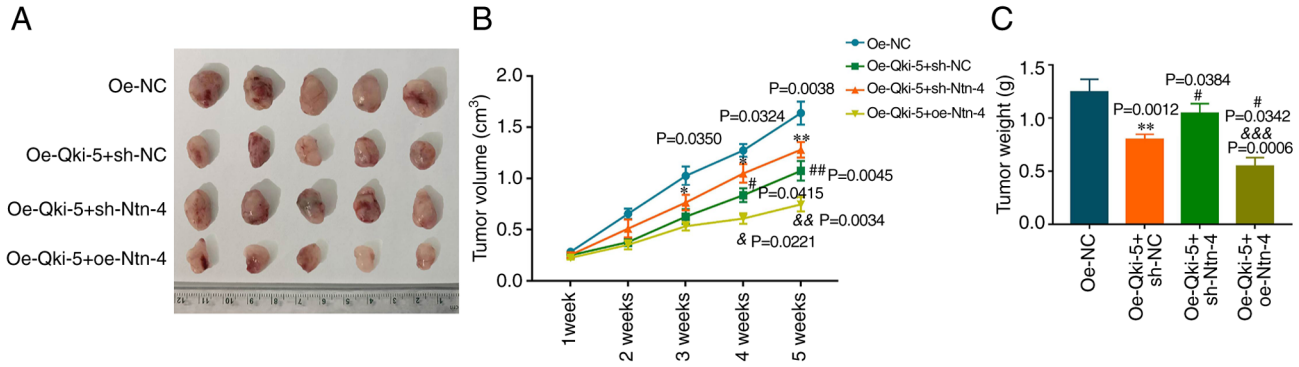

Figure 5. Qki-5 inhibits the tumorigenesis of NSCLC by upregulating Ntn-4 *in vivo*. A549 cells stably transfected with oe-NC, oe-Qki5 + sh-NC, oe-Qki5 + sh-Ntn-4 or oe-Qki5 + oe-Ntn-4 were transplanted into mice. (A) Representative images of xenograft tumours are shown. (B and C) Quantification of the tumour volumes and weights are shown. Data are presented as the mean ± SEM of three independent experiments (n=5). *P<0.05 and **P<0.01, vs. overexpression negative control (oe-NC); $^{\#}$P<0.05 and $^{\#\#}$P<0.01, vs. overexpression Qki-5 and shRNA negative control (oe-Qki-5+sh-NC); $^{\&}$P<0.05, $^{\&\&}$P<0.01 and $^{\&\&\&}$P<0.001, vs. overexpression Qki-5 and shRNA Ntn-4 (oe-Qki-5+ sh-Ntn-4); NSCLC, non-small cell lung cancer; Ntn, netrin; Qki, quaking.

overexpressed (Fig. 3M and N). Taken together, these findings indicated that Qki-5 is able to upregulate the expression level of Ntn-4 in NSCLC cells.

Qki-5 inhibits the proliferation, migration and invasion of NSCLC cells via the upregulation of Ntn-4. To investigate whether Qki-5 inhibits NSCLC progression by upregulating the expression of Ntn-4, Qki-5 was first overexpressed in A549 cells. The level of Ntn-4 was found to be increased in the cells following Qki-5 and/or Ntn-4 overexpression, whereas the level was decreased in cells following the silencing of Ntn-4 (Fig. 4A and B). Moreover, the OD values were found to be significantly decreased in the oe-Qki-5 + sh-NC group compared with the oe-NC group, although, by contrast, they were increased in the cells co-transfected with oe-Qki-5 and sh-Ntn-4. In addition, the OD values of the cells co-transfected with oe-Qki-5 and oe-Ntn-4 were found to be lower compared with those of the oe-Qki-5 + sh-NC group (Fig. 4C). The results from the scratch wound healing and Transwell assays revealed that Ntn-4 silencing was able to reverse the inhibitory effects of Qki-5 on cell migration and invasion, and both the efficiency of wound healing and the numbers of invaded cells were increased in the cells co-transfected with oe-Qki-5 and sh-Ntn-4. By contrast, the migratory and invasive capabilities of the cells were further decreased in the cells co-transfected with oe-Qki-5 and oe-Ntn-4 compared with those co-transfected with oe-Qki-5 and sh-NC (Fig. 4D and E). To further determine the role of Qki-5 and Ntn-4 in EMT, the levels of EMT marker molecules were detected, and it was found that the overexpression of Qki-5 and/or Ntn-4 led to an increase in the level of E-cadherin (Fig. 4F and G), whereas the levels of N-cadherin, vimentin and the EMT transcription factor, Snail, in A549 cells were decreased compared with the control group (Fig. 4F-J). However, by overexpressing Qki-5 and inhibiting the expression of Ntn-4 in the A549 cells, the suppressive effects of Qki-5 on EMT were found to be partly reversed (Fig. 4F-J). Subsequently, RIP assay was performed to determine whether Qki-5 is able to bind to Ntn-4 mRNA. The data obtained revealed that Ntn-4 mRNA was highly enriched in the Qki-5 antibody-precipitated RNA fraction (Fig. 4K), suggesting that Qki-5 could inhibit NSCLC progression partly by upregulating the expression of Ntn-4.

Qki-5 inhibits the tumorigenesis of NSCLC by upregulating Ntn-4 expression in vivo. To confirm the effects of Ntn-4 on tumour growth inhibition *in vivo*, the A549 cells were initially transfected with the oe-NC, oe-Qki-5 + sh-NC, oe-Qki-5 + sh-Ntn-4 or oe-Qki-5 + oe-Ntn-4 lentiviruses, and subsequently the cells were collected and subcutaneously injected into nude mice. The average volumes of the growing tumours were measured each week, and 5 weeks later, the tumours were separated and weighed. Decreases in both the volume and weight of tumours were noted in the mice injected with oe-Qki-5 + sh-NC cells compared with those in mice injected with oe-NC cells. However, the volume and weight of the tumours were increased in the mice injected with oe-Qki-5 + sh-Ntn-4 cells, whereas the cells transfected with oe-Ntn-4 and oe-Qki-5 together led to the most prominent repressive effects on tumour growth (Fig. 5).

Discussion

Over the past decade, a large number of published studies have demonstrated that alternative splicing is involved in the origin and progression of lung cancer. Alterations in particular splicing regulators result in changes in both the expression and function of their target genes in lung cancer; for example, Qki has been shown to contribute to lung cancer by regulating the splicing of the *ESYT2, NFIB, ENAH, SPAG9, NUMB* and *FN1* genes (20,28). The present study identified that the levels of Ntn-4 and Qki-5 were downregulated in lung cancer tissue and cell lines, and a high correlation existed between Ntn-4 and Qki-5. The low expression of Qki-5 suggests that it may fulfil a role in the progression of NSCLC, and that there could be an association with the poorer overall survival of patients with NSCLC. The effects of Ntn-4 on the proliferation, migration, invasion and EMT of lung cancer cells were further investigated, and it was demonstrated that the expression of Ntn-4 was regulated by Qki-5. The findings of the present study thus suggest that Ntn-4 is a potential therapeutic target for the progression of lung cancer.

It has been reported that the balance of Qki-5 and Qki-6 influences the conditions of lung cancer (29). Although both the Qki-5 and Qki-6 isoforms are detectable in lung cancer, Qki-5 is mainly expressed in tumour tissue, whereas Qki-6 is predominantly expressed in matched normal tissue in patients with NSCLC (20). Recently, several studies have shed light upon both the function and the underlying mechanisms of Qki-5 with respect to the inhibition of NSCLC progression (22-25). Circ-MTO1 serves as a 'sponge' of miR-17 to enhance the level of Qki-5, which has been found to further inhibit the Notch signalling pathway, thereby suppressing the proliferation of LUAD cells (23). At the transcriptional level, the overexpression of KLF6 has been shown to inhibit TGF-β/Smad signalling, which subsequently suppresses EMT and the invasion of LUAD mediated through the upregulation of the expression of Qki-5 (24). It has also been reported that Qki-5 can suppress the aggressiveness of NSCLC cells, either by inhibiting the β-catenin signalling pathway (22) or by alternatively suppressing the splicing of cytoskeletal gene adducing 3 (25). Consistent with the findings of the aforementioned studies, the results of the present study revealed that the mRNA and protein expression of Qki-5 was lower in lung cancer tissues compared with that in corresponding adjacent tissues. Moreover, the inhibitory effects of Qki-5 on cell proliferation, migration, invasion and EMT were confirmed by overexpressing Qki-5 in NSCLC cell lines.

As an axon guidance signal, Ntn-4 has been shown to be extensively expressed in the brain, where it contributes to multiple physiological functions in the development of the nervous system (30). In addition, Ntn-4 plays a critical role in non-nervous systems; however, the exact role(s) and mechanism(s) of Ntn-4 in different cells and tissues have yet to be fully elucidated. A high concentration of Ntn-4 (5 μg/ml) has been found to inhibit endothelial cell proliferation and promote endothelial cell apoptosis, whereas a low concentration of Ntn-4 (100 ng/ml) exerts the opposite effect (31). The majority of previously published studies have suggested that Ntn-4 binds to the receptor, Unc5B, to promote both the proliferation and differentiation of endothelial progenitor cells and the angiogenesis of ischaemic hind limbs in mice (32), whereas the proliferation and angiogenesis of human placental endothelial cells and retinas is inhibited (10,33,34). By contrast, it has been demonstrated that the role of Ntn-4 is mediated by regulating the BM through its interaction with laminin, rather than by binding to receptors of the Ntn family (13,15). Previous studies have revealed the function of Ntn-4 in several different types of tumours, including colorectal, gastric and breast cancer (9,11,15-17). In the present study, NKI data were analysed, and it was found that the level of Ntn-4 was decreased in patients with NSCLC. Furthermore, the inhibitory effects of Ntn-4 on NSCLC cell proliferation, migration and invasion were confirmed by performing gain-and-loss function experiments for Ntn-4. Of note, a study confirmed that Qki silencing suppressed the expression of Ntn-4 by directly binding to Ntn-4 mRNA in endothelial cells (35). In the present study, to clarify whether Qki-5 is able to inhibit the aggressiveness of NSCLC by regulating Ntn-4, a correlation analysis of Qki-5 and Ntn-4 was performed, which subsequently detected the expression of Ntn-4 in Qki-5-overexpressing NSCLC cells. As was anticipated, the Qki-5 mRNA level was found to be positively correlated with the level of Ntn-4 mRNA in patients with NSCLC, and the expression of Ntn-4 was upregulated in NSCLC cells overexpressing Qki-5. Furthermore, the results of RIP assay illustrated that Qki-5 could directly bind to Ntn-4 mRNA in NSCLC cells. In addition, the suppressive role of Qki-5 in the progression of NSCLC was reversed by knocking down Ntn-4 both *in vitro* and *in vivo*.

Taken together, the findings from the present study demonstrated that the levels of both Qki-5 and Ntn-4 were downregulated in patients with NSCLC and in NSCLC cell lines, and that the overexpression of Qki-5 or Ntn-4 via gene manipulation was able to suppress the proliferation, migration, invasion and EMT of NSCLC cells and tumorigenesis *in vivo*. Moreover, the inhibitory effects of Qki-5 on NSCLC progression were partly mediated via the upregulation of the expression of Ntn-4, suggesting that Ntn-4 is a target of Qki-5. In conclusion, Ntn-4 was shown to be negatively associated with NSCLC progression; therefore, it may serve as a potential biomarker for patients with NSCLC.

Acknowledgements

Not applicable.

Funding

The present study was supported by the Natural Science Foundation of Liaoning Province (grant no. 20180551268).

Availability of data and materials

The datasets used and/or analysed during the current study are available from the corresponding author on reasonable request.

Authors' contributions

ZW, SL and HJ were involved in the conception and design of the study. ZW and SL performed the experiments, collected the images, analysed the data and wrote the manuscript. SL and GP conducted the histological examination of the lung tissue, qPCR experiments and analysed the data. HJ provided funds, supervised and revised the manuscript. All authors confirmed the authenticity of all the raw data, and have read and approved the final manuscript.

Ethics approval and consent to participate

Patients diagnosed with LUAD and patients diagnosed with LUSC at the Fourth Affiliated Hospital of China Medical University were enrolled in the present study. The Ethics Committee of the Fourth Hospital of China Medical University approved the study (approval no. EC-2018-HX-013). The patients involved in this research signed informed consent forms. The animal experiments were approved by the Animal Research Ethics Committee of Animal Center of Shengjing Hospital affiliated to China Medical University (no. KT201945).

Patient consent for publication

Not applicable.

Competing interests

The authors declare that they have no competing interests.

References

1. Gazdar AF: Should we continue to use the term non-small-cell lung cancer? Ann Oncol 21 (Suppl 7): vii225-vii229, 2010.
2. Ellis PM and Vandermeer R: Delays in the diagnosis of lung cancer. J Thorac Dis 3: 183-188, 2011.
3. Cirulli V and Yebra M: Netrins: Beyond the brain. Nat Rev Mol Cell Biol 8: 296-306, 2007.
4. Yurchenco PD and Wadsworth WG: Assembly and tissue functions of early embryonic laminins and netrins. Curr Opin Cell Biol 16: 572-579, 2004.
5. Bruikman CS, Zhang H, Kemper AM and van Gils JM: Netrin family: Role for protein isoforms in cancer. J Nucleic Acids 2019: 3947123, 2019.
6. Ziegon L and Schlegel M: Netrin-1: A modulator of macrophage driven acute and chronic inflammation. Int J Mol Sci 23: 275, 2021.
7. Nacht M, St Martin TB, Byrne A, Klinger KW, Teicher BA, Madden SL and Jiang Y: Netrin-4 regulates angiogenic responses and tumor cell growth. Exp Cell Res 315: 784-794, 2009.
8. Eveno C, Broqueres-You D, Feron JG, Rampanou A, Tijeras-Raballand A, Ropert S, Leconte L, Levy BI and Pocard M: Netrin-4 delays colorectal cancer carcinomatosis by inhibiting tumor angiogenesis. Am J Pathol 178: 1861-1869, 2011.
9. Eveno C, Contreres JO, Hainaud P, Nemeth J, Dupuy E and Pocard M: Netrin-4 overexpression suppresses primary and metastatic colorectal tumor progression. Oncol Rep 29: 73-78, 2013.
10. Lejmi E, Leconte L, Pedron-Mazoyer S, Ropert S, Raoul W, Lavalette S, Bouras I, Feron JG, Maitre-Boube M, Assayag F, *et al*: Netrin-4 inhibits angiogenesis via binding to neogenin and recruitment of Unc5B. Proc Natl Acad Sci USA 105: 12491-12496, 2008.
11. Lv B, Song C, Wu L, Zhang Q, Hou D, Chen P, Yu S, Wang Z, Chu Y, Zhang J, *et al*: Netrin-4 as a biomarker promotes cell proliferation and invasion in gastric cancer. Oncotarget 6: 9794-9806, 2015.
12. Villanueva AA, Falcon P, Espinoza N, R LS, Milla LA, Hernandez-SanMiguel E, Torres VA, Sanchez-Gomez P and Palma V: The Netrin-4/Neogenin-1 axis promotes neuroblastoma cell survival and migration. Oncotarget 8: 9767-9782, 2017.
13. Reuten R, Patel TR, McDougall M, Rama N, Nikodemus D, Gibert B, Delcros JG, Prein C, Meier M, Metzger S, *et al*: Structural decoding of netrin-4 reveals a regulatory function towards mature basement membranes. Nat Commun 7: 13515, 2016.
14. Mehlen P and Fattet L: Netrin-4 regulates stiffness and metastasis. Nat Mater 20: 722-723, 2021.
15. Reuten R, Zendehroud S, Nicolau M, Fleischhauer L, Laitala A, Kiderlen S, Nikodemus D, Wullkopf L, Nielsen SR, McNeilly S, *et al*: Basement membrane stiffness determines metastases formation. Nat Mater 20: 892-903, 2021.
16. Esseghir S, Kennedy A, Seedhar P, Nerurkar A, Poulsom R, Reis-Filho JS and Isacke CM: Identification of NTN_4, TRA_1, and STC_2 as prognostic markers in breast cancer in a screen for signal sequence encoding proteins. Clin Cancer Res 13: 3164-3173, 2007.
17. Yi L, Lei Y, Yuan F, Tian C, Chai J and Gu M: NTN4 as a prognostic marker and a hallmark for immune infiltration in breast cancer. Sci Rep 12: 10567, 2022.
18. Chenard CA and Richard S: New implications for the QUAKING RNA binding protein in human disease. J Neurosci Res 86: 233-242, 2008.
19. Biedermann B, Hotz HR and Ciosk R: The Quaking family of RNA-binding proteins: Coordinators of the cell cycle and differentiation. Cell Cycle 9: 1929-1933, 2010.
20. de Miguel FJ, Pajares MJ, Martinez-Terroba E, Ajona D, Morales X, Sharma RD, Pardo FJ, Rouzaut A, Rubio A, Montuenga LM and Pio R: A large-scale analysis of alternative splicing reveals a key role of QKI in lung cancer. Mol Oncol 10: 1437-1449, 2016.
21. Zhang H, Li J, Tian F, Su X, Wang X, Tang D, Zhang L, Zhang T and Ni Y: QKI-6 suppresses cell proliferation, migration, and emt in non-small cell lung cancer. Front Oncol 12: 897553, 2022.
22. Zhou X, Li X, Sun C, Shi C, Hua D, Yu L, Wen Y, Hua F, Wang Q, Zhou Q and Yu S: Quaking-5 suppresses aggressiveness of lung cancer cells through inhibiting β-catenin signaling pathway. Oncotarget 8: 82174-82184, 2017.
23. Zhang B, Chen M, Jiang N, Shi K and Qian R: A regulatory circuit of circ-MTO1/miR-17/QKI-5 inhibits the proliferation of lung adenocarcinoma. Cancer Biol Ther 20: 1127-1135, 2019.
24. Wang S, Tong X, Li C, Jin E, Su Z, Sun Z, Zhang W, Lei Z and Zhang HT: Quaking 5 suppresses TGF-β-induced EMT and cell invasion in lung adenocarcinoma. EMBO Rep 22: e52079, 2021.
25. Wang JZ, Fu X, Fang Z, Liu H, Zong FY, Zhu H, Yu YF, Zhang XY, Wang SF, Huang Y and Hui J: QKI-5 regulates the alternative splicing of cytoskeletal gene ADD3 in lung cancer. J Mol Cell Biol 13: 347-360, 2021.
26. Li N, Deng CL, Zhang B and Ye HQ: Viral titer quantification of west nile virus by immunostaining plaque assay. Methods Mol Biol 2585: 15-21, 2023.
27. Livak KJ and Schmittgen TD: Analysis of relative gene expression data using real-time quantitative PCR and the 2(-Delta Delta C(T)) method. Methods 25: 402-408, 2001.
28. Coomer AO, Black F, Greystoke A, Munkley J and Elliott DJ: Alternative splicing in lung cancer. Biochim Biophys Acta Gene Regul Mech 1862: 194388, 2019.
29. Sebestyen E, Zawisza M and Eyras E: Detection of recurrent alternative splicing switches in tumor samples reveals novel signatures of cancer. Nucleic Acids Res 43: 1345-1356, 2015.
30. Staquicini FI, Dias-Neto E, Li J, Snyder EY, Sidman RL, Pasqualini R and Arap W: Discovery of a functional protein complex of netrin-4, laminin gamma1 chain, and integrin alpha-6beta1 in mouse neural stem cells. Proc Natl Acad Sci USA 106: 2903-2908, 2009.
31. Han Y, Shao Y, Liu T, Qu YL, Li W and Liu Z: Therapeutic effects of topical netrin-4 inhibits corneal neovascularization in alkali-burn rats. PLoS One 10: e0122951,2015.
32. Lee NG, Jeung IC, Heo SC, Song J, Kim W, Hwang B, Kwon MG, Kim YG, Lee J, Park JG, *et al*: Ischemia-induced Netrin-4 promotes neovascularization through endothelial progenitor cell activation via Unc-5 Netrin receptor B. FASEB J 34: 1231-1246, 2020.
33. Dakouane-Giudicelli M, Brouillet S, Traboulsi W, Torre A, Vallat G, Si Nacer S, Vallée M, Feige JJ, Alfaidy N and de Mazancourt P: Inhibition of human placental endothelial cell proliferation and angiogenesis by netrin-4. Placenta 36: 1260-1265, 2015.
34. Kociok N, Crespo-Garcia S, Liang Y, Klein SV, Nurnberg C, Reichhart N, Skosyrski S, Moritz E, Maier AK, Brunken WJ, *et al*: Lack of netrin-4 modulates pathologic neovascularization in the eye. Sci Rep 6: 18828, 2016.
35. Zhang H, Vreeken D, Leuning DG, Bruikman CS, Junaid A, Stam W, de Bruin RG, Sol WMPJ, Rabelink TJ, van den Berg BM, *et al*: Netrin-4 expression by human endothelial cells inhibits endothelial inflammation and senescence. Int J Biochem Cell Biol 134: 105960, 2021.